

## Variational approach for calculating Auger electron spectra: Going beyond the impurity approximation

Anamitra Mukherjee,<sup>1</sup> George A. Sawatzky,<sup>1,2,3</sup> and Mona Berciu<sup>1,2</sup>

<sup>1</sup>*Department of Physics and Astronomy, University of British Columbia, Vancouver, British Columbia, Canada, V6T 1Z1*

<sup>2</sup>*Quantum Matter Institute, University of British Columbia, Vancouver, British Columbia, Canada, V6T 1Z4*

<sup>3</sup>*Department of Chemistry, University of British Columbia, Vancouver, British Columbia, Canada, V6T 1Z1*

(Received 17 January 2013; published 29 April 2013)

We propose a variational method to calculate the two-hole propagators relevant for Auger spectroscopy in transition-metal oxides. This method can be thought of as an intermediary step between the full solution (which is difficult to generalize to systems with partially filled bands) and the impurity approximation. Like the former, our solution has full translational invariance, and like the latter, it can be generalized to certain types of systems with partially filled bands. Here we compare both our variational approximation and the impurity approximation against the exact solution for a simple one-dimensional model with filled bands. We show that when the energies of the eigenstates residing primarily on the transition-metal ions do not overlap with those of the eigenstates residing primarily on oxygen ions, both approximations are valid but the variational approach is superior.

DOI: [10.1103/PhysRevB.87.165136](https://doi.org/10.1103/PhysRevB.87.165136)

PACS number(s): 82.80.Pv, 71.27.+a

### I. INTRODUCTION

Spectroscopic measurements are a powerful set of tools for probing various aspects of many-body physics.<sup>1,2</sup> Among these, Auger electron spectroscopy (AES) provides information about the local atomic multiplet structure, on-site interaction strengths, and the crystal fields.<sup>3–5</sup> In transition-metal oxides, the AES of the transition element can be supplemented by the O *KLL* Auger spectra, resulting in additional information about the O on-site repulsion energy as well as interactions between holes located on nearest-neighbor transition-metal and O ions.<sup>6</sup> Such information is vital for understanding correlated materials, which is why AES has been the subject of sustained research for a long time.

The Auger process consists of the decay of a core hole into two final-state holes (initially located at the atomic site where the original core hole was created by the high-energy x ray) plus an Auger electron, and is mediated by on-site Coulomb interactions. One of the most studied cases has these two final-state holes residing in the valence band and goes by the name of core-valence-valence (CVV) Auger spectroscopy. From a theoretical point of view, the easiest case to handle has a full valence band except for the two Auger holes. The central quantity of interest is the two-hole Green's function, which for an otherwise full band can be calculated within the two-step approximation using the Cini-Sawatzky theory.<sup>7–9</sup> The resulting two-hole spectral function, multiplied by momentum-dependent matrix element factors, provides the theoretical predictions for AES.<sup>10</sup> Many extensions have been proposed to incorporate various aspects such as dynamical screening,<sup>11–13</sup> off-site interactions,<sup>14</sup> overlap effects,<sup>15–17</sup> and one-step formulation.<sup>18</sup> We refer the reader to a recent review<sup>19</sup> for more details. These efforts have led to spectacular success in explaining AES for materials such as Cu and Cu<sub>2</sub>O.

However, the problem of understanding AES for systems with a partially filled valence band, such as the oxides of transition elements Ni, Co, Fe, Mn, etc., remains open because the two-hole spectral function is very challenging

to compute in this case. This is because in the presence of other holes the dynamics of the two additional holes is a complicated many-body problem, whereas in an otherwise full band the two holes interact only with one another (if we ignore electron-hole excitations between the valence and the conduction bands), i.e., this is a two-body problem. Limited success has been achieved employing variants of the bare ladder approximations<sup>20</sup> and assuming low hole density in the bands. A completely different approach is to use the Anderson impurity approximation, whose underlying idea is as follows: in transition-metal (TM) oxides, the transition-metal atoms are typically connected to each other through oxygen ligands. The simplest example in one dimension is sketched in Fig. 1(a), and has transition-metal atoms intercalated with O atoms. In the impurity approximation,<sup>21–24</sup> the full problem is simplified to that of a single transition-metal atom coupled to the bath of O, as sketched in Fig. 1(b). This greatly simplifies the calculation and is a reasonable step towards understanding local multiplet structures. However, because the symmetry of the problem is lowered, momentum-resolved spectral weights cannot be calculated.

Here, we propose a variational approach for finding the two-hole Green's functions needed for AES, which can be thought of as an intermediary step between the impurity approximation and the full lattice calculation. Like the former, it has a reduced Hilbert space and can therefore be generalized to (some) systems with partially filled bands. Like the latter, it has full translational invariance so that momentum-resolved spectral weights can be calculated. We argue that the location of the spectral weight component ignored within our approximation can be inferred *a priori*, but should be small for materials where AES is a useful probe. Moreover, the variational space can be systematically enlarged to check the relevance of some of the neglected terms.

In this paper, we present the underlying idea and the general formalism of this variational approach, which is based on a recently developed method to calculate many-particle Green's functions.<sup>25–27</sup> Here, we apply it to the simple model sketched in Fig. 1 and assume otherwise full bands, so that we

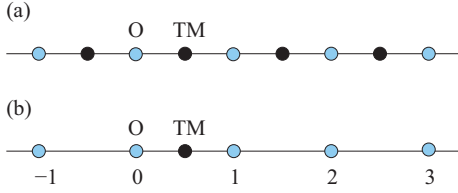


FIG. 1. (Color online) (a) Sketch of the one-dimensional (1D) periodic Anderson model. TM and O represent transition-metal and O ions, respectively. (b) In the impurity approximation, an impurity TM ion is coupled to the 1D “bath” of O.

can benchmark it against the exact solution available in this case. For completeness, we also show impurity approximation results for this model. This allows us to gauge the advantages and disadvantages of both of these approximations and to understand for what regions in the parameter space they are valid. This information will guide us, in future work, to use this method for appropriate systems where the transition elements have partially filled  $d$  orbitals.

The paper is organized as follows. In Sec. II we define the Hamiltonians and in Sec. III we discuss the methods to calculate two-hole propagators exactly and with the two approximations. In Sec. IV, we present the exact results and compare them with those predicted by our variational approximation as well as the impurity approximation for two different topologies of coupling between the impurity and the bath of O. Section V contains the summary and conclusions. Some of the details are presented in the two Appendices.

## II. HAMILTONIAN

### A. The periodic Anderson model

The periodic one-dimensional (1D) Anderson model shown in Fig. 1(a) is defined by the Hamiltonian

$$\mathcal{H}_P = \mathcal{H}_{\text{TM}} + \mathcal{H}_O + \mathcal{H}_{\text{hyb}},$$

where  $\mathcal{H}_{\text{TM}}$  describes the TM atoms, which for simplicity are assumed to have only two (spin-degenerate) states each, and is given by

$$\mathcal{H}_{\text{TM}} = U \sum_i n_{d,i,\uparrow} n_{d,i,\downarrow} + \Delta \sum_{i,\sigma} n_{d,i,\sigma}.$$

The O “bath” is described by a 1D Hubbard model,

$$\mathcal{H}_O = -t \sum_{i,\sigma} (c_{i,\sigma}^\dagger c_{i+1,\sigma} + \text{H.c.}) + U_O \sum_i n_{i,\uparrow} n_{i,\downarrow},$$

while the TM-O hybridization is described by

$$\mathcal{H}_{\text{hyb}} = -V \sum_{i,\sigma} [d_{i,\sigma}^\dagger (c_{i,\sigma} + c_{i-1,\sigma}) + \text{H.c.}].$$

Here, all creation operators are electron creation operators, with  $c_{i\sigma}$  and  $d_{i\sigma}$  the operators for O and TM orbitals, respectively, with the convention that the  $i$ th TM atom is placed to the left of the  $i$ th O atom. As usual,  $n_{d,i,\sigma} = d_{i\sigma}^\dagger d_{i\sigma}$ ,  $n_{i\sigma} = c_{i\sigma}^\dagger c_{i\sigma}$ . For bookkeeping purposes, we assume that there are  $N$  TM and  $N$  O sites, but in the final calculation, we let

$N \rightarrow \infty$ . Because the method we introduce below is based on a real-space representation, the addition of longer-range interactions, such as repulsion between holes residing on neighboring TM and O sites, is trivial to implement. This model assumes that only the  $\sigma$ -bonding O  $2p$  orbitals pointing towards the TM neighbors are relevant. Generalization to models that include more O and/or TM orbitals, as well as lattices in higher dimensions, is discussed below.

For AES in a system with full bands, we start from the completely full ground state  $|\Omega\rangle_P = \prod_{i,\sigma} d_{i,\sigma}^\dagger c_{i,\sigma}^\dagger |0\rangle$  of energy  $E_\Omega^P = N(2\Delta + U + U_O)$ , and create two holes. Because the periodic Hamiltonian is invariant to translations and because we want to describe states where the two holes can be at the same site, we choose two-hole basis states with a total momentum  $k$  and zero-spin projection,<sup>25</sup> namely,  $|k,n,dd\rangle = \frac{1}{\sqrt{N}} \sum_i e^{ik(R_i+na/2)} d_{i,\uparrow} d_{i+n,\downarrow} |\Omega\rangle_P$  if both holes are on TM sites,  $|k,n,dc\rangle = \frac{1}{\sqrt{N}} \sum_i e^{ik(R_i+na/2)} d_{i,\uparrow} c_{i+n,\downarrow} |\Omega\rangle_P$  and  $|k,n,cd\rangle = \frac{1}{\sqrt{N}} \sum_i e^{ik(R_i+na/2)} c_{i,\uparrow} d_{i+n,\downarrow} |\Omega\rangle_P$  if one hole is on a TM site and the other is at an O site, and finally  $|k,n,cc\rangle = \frac{1}{\sqrt{N}} \sum_i e^{ik(R_i+na/2)} c_{i,\uparrow} c_{i+n,\downarrow} |\Omega\rangle_P$  if both holes are in the O bath. Here,  $a$  is the lattice constant and  $n = -\frac{N}{2} + 1, \dots, \frac{N}{2}$  takes all possible values consistent with the periodic boundary conditions. Taken together, these states constitute a full basis for the Hilbert subspace containing states with total momentum  $k$  and zero-spin projection.

The aim is to find the propagator

$$G_{dd}(k,0,\omega) = \langle k,0,dd | \hat{G}_P(\omega) | k,0,dd \rangle,$$

where  $\hat{G}_P(\omega) = [\omega + i\eta - (\mathcal{H}_P - E_\Omega^P)]^{-1}$  is the resolvent for  $\mathcal{H}_P$  because its associated spectral weight  $A_{dd}(k,0,\omega) = -\frac{1}{\pi} \text{Im}[G_{dd}(k,0,\omega)]$ , which has poles at energies  $\omega = E_{2h}(k) - E_\Omega^P$  for any two-hole eigenstate with total momentum  $k$  and energy  $E_{2h}(k)$ , is proportional to the momentum-resolved spectral intensity measured by AES. As discussed below, our solution also provides the values of many other propagators beside  $G_{dd}(k,0,\omega)$ , from which other useful information can be gleaned.

### B. Anderson impurity problem

The impurity approximation is a variational approximation where the holes are not allowed on any TM ions apart from the original one; this is equivalent to excluding all such orbitals from the variational space. As a result, the full periodic problem is reduced to the Anderson impurity problem sketched in Fig. 1(b), and its Hamiltonian becomes

$$\mathcal{H}_I = \mathcal{H}_{\text{TM},I} + \mathcal{H}_O + \mathcal{H}_{\text{hyb},I},$$

where

$$\mathcal{H}_{\text{TM},I} = U n_{d,\uparrow} n_{d,\downarrow} + \Delta \sum_\sigma n_{d,\sigma}$$

describes the impurity TM site, the O bath is described by  $\mathcal{H}_O$  as before, and

$$H_{\text{hyb},I} = -V \sum_\sigma [d_\sigma^\dagger c_{1,\sigma} + d_\sigma^\dagger c_{0,\sigma} + \text{H.c.}]$$

is their hybridization, with the impurity taken to be located between the bath O labeled 0 and 1. Here, again, all operators

are electron operators and  $d_\sigma^\dagger$  is the creation operator for the orbital of the TM impurity site.

The filled-band ground state is now  $|\Omega\rangle_I = \prod_\sigma d_\sigma^\dagger \prod_i c_{i,\sigma}^\dagger |0\rangle$  and its corresponding energy is  $E_\Omega^I = 2\Delta + U + NU_O$ . To calculate AES-relevant spectra, we consider two-hole excitations in this ground state by removing two electrons with opposite spins. Since invariance to translations is lost, the generic real-space states of interest are now  $|\sigma, j\sigma'\rangle \equiv c_{i\sigma} c_{j\sigma'} |\Omega\rangle_I, |d\sigma, i\sigma'\rangle = d_\sigma c_{i\sigma'} |\Omega\rangle_I$ , and  $|dd\rangle = d_\uparrow d_\downarrow |\Omega\rangle_I$ . Now we are primarily interested in calculating the two-hole impurity Green's function  $G_{dd}(\omega) = \langle dd | \hat{G}_I(\omega) | dd \rangle$ , where  $\hat{G}_I(\omega) = [\omega + i\eta - (\mathcal{H}_I - E_\Omega^I)]^{-1}$ , and its corresponding two-hole spectral function  $A_{dd}(\omega) = -\frac{1}{\pi} \text{Im}[G_{dd}(\omega)]$ .

### III. METHOD

We begin with the exact solution for the periodic Anderson model. To find the propagator of interest to us,  $G_{dd}(k, 0, \omega)$ , we generate its equation of motion (EOM) from the identity  $\hat{G}_P(\omega)(\omega - \mathcal{H}_P + E_\Omega^P + i\eta) = \hat{I}$ . Calculating its diagonal matrix element for  $|k, 0, dd\rangle$ , we find

$$\begin{aligned} & (\omega + 2\Delta + U + i\eta)G_{dd}(k, 0, \omega) \\ &= 1 + V \left[ e^{\frac{ika}{2}} G_{cd}(k, 1, \omega) + G_{cd}(k, 0, \omega) \right. \\ & \quad \left. + e^{\frac{ika}{2}} G_{dc}(k, -1, \omega) + G_{dc}(k, 0, \omega) \right], \end{aligned}$$

where  $G_{\alpha\beta}(k, n, \omega) = \langle k, 0, dd | \hat{G}_P(\omega) | k, n, \alpha\beta \rangle$  for  $\alpha, \beta = c, d$ . In other words, because the Hamiltonian links the state  $|k, 0, dd\rangle$  to states with one hole on a TM site and one on a neighboring O, the EOM links  $G_{dd}(k, 0, \omega)$  to propagators corresponding to such states. Their EOM can be generated similarly, and we obtain an infinite sequence of coupled linear equations.

To solve it, we couple the propagators with holes at the same distance  $n$  in a vector,

$$V_n = \begin{pmatrix} G_{dd}(k, n, \omega) \\ G_{dc}(k, n, \omega) \\ G_{cd}(k, n, \omega) \\ G_{cc}(k, n, \omega) \end{pmatrix},$$

and note that for any  $n \neq 0$ , the EOM can be grouped in the simple recurrence relation

$$\gamma_n V_n = \beta_n V_{n+1} + \alpha_n V_{n-1}$$

for any given  $k$  and  $\omega$ . Here,  $\gamma_n$ ,  $\beta_n$ , and  $\alpha_n$  are simple  $4 \times 4$  matrices that are read off directly from the EOM. We note that one can always group the EOM in such simple recurrence relations, even for models which allow longer-range hopping<sup>26</sup> and/or in higher dimensions.<sup>27</sup> For  $n = 0$ , the recurrence relation also has an inhomogeneous term,

$$\gamma_0 V_0 = X + \beta_0 V_1 + \alpha_0 V_{-1},$$

where  $X^T = (1, 0, 0, 0)$  for this problem. The solution of such recurrence relations has been discussed extensively elsewhere.<sup>25-27</sup> Briefly, we must have  $V_n \rightarrow 0$  as  $|n| \rightarrow \infty$  because the Fourier transform of these propagators are the amplitudes of probability to have the two holes evolve from

being on the same TM site to being  $n$  sites away from each other, in a given time. As  $|n| \rightarrow \infty$ , this becomes very unlikely, and the presence of the broadening  $\eta$  which introduces an artificial lifetime  $1/\eta$  makes it even less so. As a result, for  $n \geq 1$ , we have  $V_n = A_n(k, \omega)V_{n-1}$ , where  $A_n = [\gamma_n - \beta_n A_{n+1}]^{-1} \alpha_n$  is calculated starting with  $A_M = 0$  for a sufficiently large cutoff  $M$ . Similarly, for  $n \leq -1$ , we have  $V_n = B_n(k, \omega)V_{n+1}$ , where  $B_n = [\gamma_n - \alpha_n A_{n-1}]^{-1} \beta_n$  is calculated starting with  $B_{-|M|} = 0$ . Using  $V_1 = A_1 V_0$  and  $V_{-1} = B_{-1} V_0$  in the  $n = 0$  equation gives

$$V_0 = [\gamma_0 - \beta_0 A_1(k, \omega) - \alpha_0 B_{-1}(k, \omega)]^{-1} X.$$

This gives us  $G_{dd}(k, 0, \omega)$  as the top entry in  $V_0$ . All other  $n = 0$  propagators, as well as those with  $|n| < M$ , can also then be calculated efficiently. Projecting on a different state than  $\langle k, 0, dd |$  simply requires using a different  $X$ , so other propagators can be found easily.

In principle, this method generalizes straightforwardly to lattices in any dimension and with any topology, so no approximations should be necessary. In practice, however, the computational cost quickly becomes prohibitive. For instance, for models with nearest-neighbor hopping in higher dimensions, one must group together in  $V_n$  all propagators where the holes are separated by  $n_x a \hat{e}_x + n_y a \hat{e}_y + \dots$  with  $|n_x| + |n_y| + \dots = n$ , i.e., with the same Manhattan distance.<sup>27</sup> As a result, the dimension of  $V_n$  increases roughly like  $n^{d-1}$ . Adding more orbitals at the TM/O sites will further amplify the problem by increasing in a combinatorial fashion the number of possible propagators with the same  $(n_x, n_y, \dots)$  separation. As a result, while the solution can still be cast in terms of continued fractions of matrices, their dimensions increase quickly with  $n$ , resulting in significant computational costs. This is why efficient approximations are needed.

As already mentioned, one much-employed option is the impurity approximation. Its solution for  $G_{dd}(\omega)$  can also be formulated in terms of continued fractions of matrices (we present the details in the Appendix, since we are not aware of a prior similar solution for this problem). This approximation reduces the number of possible propagators by removing all but one TM site from the problem. As a result, there is now only one state with both holes at the impurity TM site, as opposed to  $N^2$  in the full periodic problem (i.e., including all allowed total momenta), and only  $2N$  combinations with one hole at the TM and one at an O site, as opposed to  $2N^2$  options in the full problem. The number of states associated with both holes in the O bath is not changed.

The total number of distinct propagators is therefore reduced from  $4N^2$  in the full problem to  $(N+1)^2$  in the impurity limit, suggesting that the latter is considerably more efficient. However, the full problem can be solved individually for each of the allowed  $N$  total momenta, since the translational invariance guarantees that propagators with different momenta do not mix. Thus, one needs to solve  $N$  distinct problems with  $4N$  propagators each, as discussed above. In the impurity problem, loss of translational invariance means that all propagators are coupled to one another through the EOM. From this perspective, it is far less clear that using the impurity approximation is computationally more efficient, although to fully settle this, one needs to take into account

all other possible symmetries and the effects of the truncation (for large system, the cutoff  $M \ll N/2$ ). In practice, the O bath is often replaced by a featureless density of states (we do not make this further approximation in our calculations). This certainly makes the impurity problem very efficient, but it also loses all information regarding the role of the O bath topology, on top of the loss of ability to momentum resolve the AES spectral weights.

From this analysis, it is clear that a better strategy would be to lower the total number of propagators while maintaining translational invariance. This is the basis for our proposed variational method. Our proposal is to remove the propagators which have the holes at different TM sites. This is equivalent to excluding these states from the Hilbert space, which is why this is a variational approximation. Mathematically, this is easily achieved by setting  $G_{dd}(k, n, \omega) \equiv 0$  for all  $n \neq 0$  in the EOM discussed above, leading to vectors  $V_n$ ,  $n \neq 0$  of dimension three instead of four. Of course, the saving is not big for this simple case, but it becomes considerable in higher dimensions and/or for more TM orbitals. Because its variational space is significantly larger than that of the impurity approximation, this method is also guaranteed to be more accurate.

Physically, what this means is that both holes start at the same (any) TM site. Eventually, both hop into the O bath and move through the system, but whenever they happen to both hop back to TM sites they must go to the same TM ion. For systems with strong correlations, i.e., where the states with the holes at the same TM site are at quite different energies from states with the holes at different TM sites, this should be a reasonable approach and is close to the intuitive picture of what happens in AES. In a way, one could view this as a “lattice of impurities.” Besides maintaining translational invariance, this method has the added benefit that we can infer *a priori* the effect of removing these states, as we discuss in the next section. Moreover, if need be, one can also systematically add some of these states back into the calculation—for example, starting with the states where the holes belong to neighboring TM sites only. Their importance can therefore be assessed quantitatively. Generalization to systems with partially filled TM orbitals is also less computationally costly than for the full solution. More discussion on the meaning and relevance of this approximation is presented below.

## IV. RESULTS

### A. The periodic Anderson model

We start by discussing the full periodic model. Besides providing the test case against which we compare the variational and the impurity approximations, this also allows us to understand the various features of these spectra and their dependence on the various parameters. Since the origin of some of these various features is model independent (for example, the location of the continua in the AES spectrum is always obtained from the self-convolution of the one-hole spectrum), spectra with qualitatively similar features should be expected in more realistic models.

To understand the dependence of the AES spectral weight  $A_{dd}(k, 0, \omega)$  on the various parameters, we start by setting

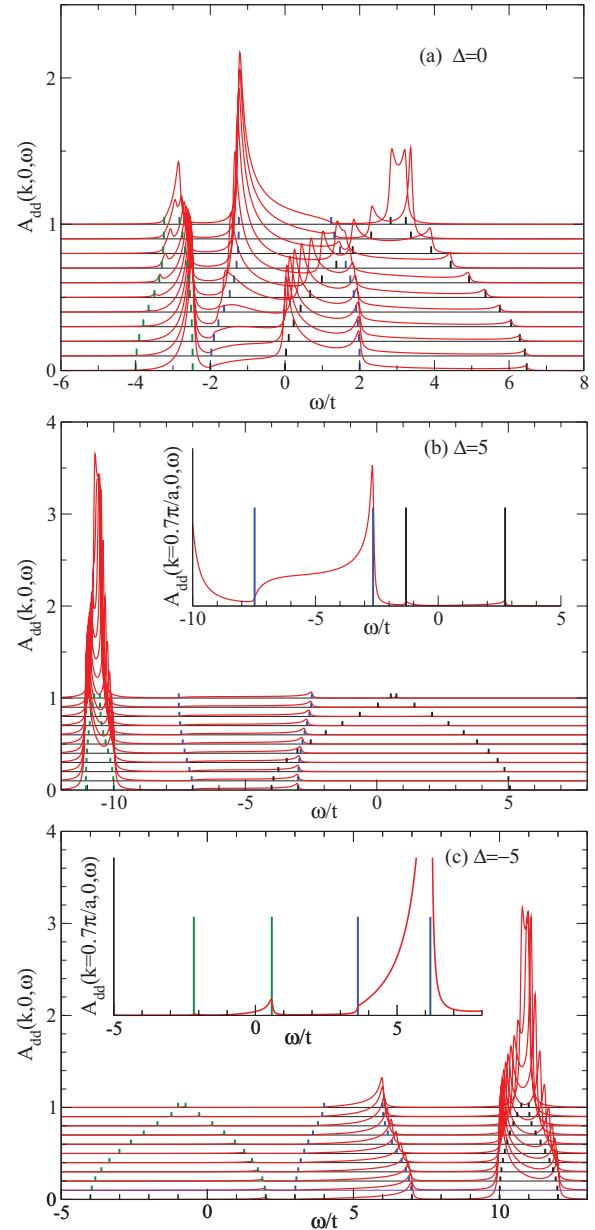


FIG. 2. (Color online) AES spectral weights  $A_{dd}(k, 0, \omega)$  for the full periodic model vs  $\omega$  for  $k \in [0, \pi/a]$ . The curves are shifted vertically with increasing  $k$ . In all cases,  $t = V = 1$ ,  $U = U_O = 0$ ,  $\eta = 0.05$ , while (a)  $\Delta = 0$ , (b)  $\Delta = 5$ , and (c)  $\Delta = -5$ . The small vertical lines indicated the expected locations of band edges. See text for more details.

$U = U_O = 0$ ,  $t = V = 1$ , and varying  $\Delta$ . Momentum-resolved results are shown in Fig. 2 for uniformly spaced values of  $k$  from 0 to  $\pi/a$ .

To make sense of these fairly complicated spectra, we note that these parameters correspond to a noninteracting system. As a result, the two-hole spectra must be convolutions of single-hole spectra, which are easy to calculate (note that single-hole spectra can also be obtained experimentally from angle-resolved photoemission). Straightforward calculations show that a hole of momentum  $k$  introduced in the state  $|\Omega\rangle_p$

has two possible eigenenergies:

$$E_{1h}^{(\pm)}(k) = \frac{1}{2} \left\{ -U - \Delta - U_O + 2t \cos(ka) \pm \sqrt{[U + \Delta - U_O + 2t \cos(ka)]^2 + 16V^2 \cos^2 \frac{ka}{2}} \right\}. \quad (1)$$

If  $\Delta$  is sufficiently large, these correspond to either having the hole preponderantly on the TM sites (i.e., a TM-like band) or in an O-like band. Note that the electron correlation energies  $U, U_O$  enter here because the single hole is introduced in an otherwise full band.

The convolution of these two one-hole continua result in three two-hole continua, covering the ranges  $E_{2h}^{(\gamma\delta)}(k) \in \{E_{1h}^{(\gamma)}(k-q) + E_{1h}^{(\delta)}(q) | -\frac{\pi}{a} < q \leq \frac{\pi}{a}\}$  for  $\delta, \gamma = \pm$ . Their band edges are shown by small vertical markers in Fig. 2; each band has a different color. These expected band edges indeed agree perfectly with the features seen in the AES spectral weight (a broadening  $\eta = 0.05$  was used in the spectral weight, accounting for the apparent ‘‘overflow’’ at band edges).

For  $\Delta = 0$ , the two upper bands overlap partially, and the spectral weight is distributed fairly equally between all features. For  $\Delta = \pm 5$ , most of the weight is in the lowest/highest continuum which contains states with both holes in the TM-like band and thus has the highest overlap with the state  $|k, 0, dd\rangle$  of interest to AES. This band is centered at  $-2\Delta$ , which is the change in energy if two holes are removed from TM sites if there was no hybridization,  $V = 0$ , and in the absence of correlations,  $U = U_O = 0$ , and is fairly narrow since the holes cannot hop directly between TM sites. The middle continuum, with one hole in the TM-like band and one in the O-like band, has less weight but is still visible. It is centered around  $-\Delta$ , i.e., the energy cost for removing one electron from the TM site, and is broader because the O-like band has significant bandwidth. The third continuum, with both holes in the O-like band, has very little overlap with the state  $|k, 0, dd\rangle$  and is therefore only visible when the scale is significantly expanded, as shown in the insets. It is centered around the origin (for  $U_O = 0$ ) and is the broadest of the three features because holes can hop directly between O sites. In the limit  $V \rightarrow 0$ , the maximum bandwidth of this continuum should be  $8t$ , when  $k = 0$ . We see that hopping on and off the TM sites, controlled by  $V$ , has a significant influence on this bandwidth when  $V \sim t$ .

While one can set any values for parameters in a theoretical study, physically it makes sense to focus on cases where the low-energy states favor having the extra holes at the TM sites, so that AES is maximally sensitive to the TM parameters. Simple arguments, listed in Appendix B, show that this implies  $\Delta > 2t + U_O$ .

As a result, we set  $\Delta = 5$  and investigate the role of the on-site correlations. Figure 3(a) shows  $A_{dd}(k, 0, \omega)$  for  $U = 5, U_O = 0$ , while Fig. 3(b) is for  $U = 5, U_O = 3$ . Comparing Fig. 3(a) with Fig. 2(b), we see that the lowest band with the two holes in the TM-like bands has shifted by about  $2U$  and is now centered around  $-2(\Delta + U)$ , as expected since  $-(\Delta + U)$  is the energy cost for removing an electron from a TM site (if there was no hybridization with the O bath).

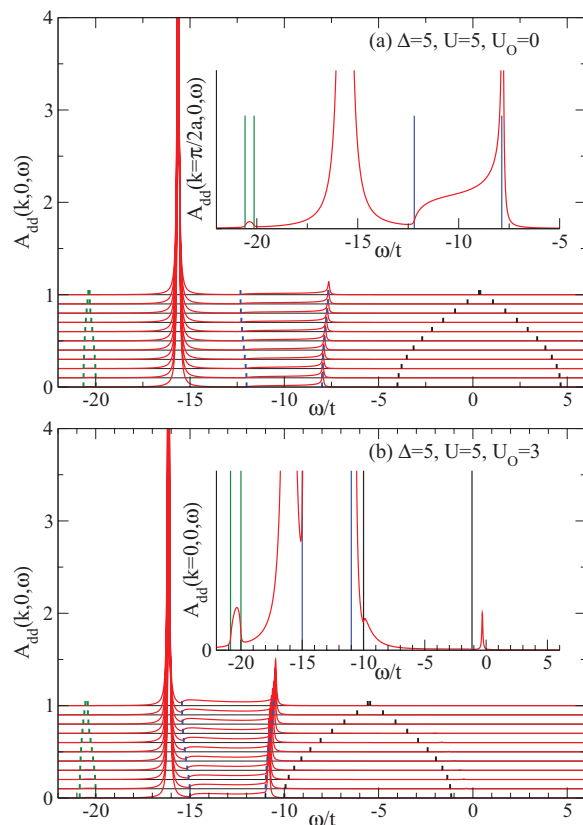


FIG. 3. (Color online) AES spectral weights for the full periodic model  $A_{dd}(k, 0, \omega)$  vs  $\omega$  for  $k \in [0, \pi/a]$ . The curves are shifted vertically with increasing  $k$ . In all cases,  $t = V = 1$ ,  $\Delta = 5$ ,  $\eta = 0.05$ , while (a)  $U = 5, U_O = 0$  and (b)  $U = 5, U_O = 3$ . The small vertical lines indicated the expected locations of band edges. See text for more details.

Similarly, the middle band is shifted by about  $U$  to around  $-\Delta - U$ , while the upper band with the two holes in the O bath is essentially unchanged. Apart from these expected shifts, we see that most spectral weight has moved from the lowest band (where it was for  $U = 0$ ) into a new discrete peak that has appeared  $\sim U$  above it. This weakly dispersing peak describes (anti)bound states with both holes at the same TM site, hence the large overlap with  $|k, 0, dd\rangle$ . Indeed, it is located close to  $-2\Delta - U$ , where it would be expected to appear in the absence of hybridization with the O bath. For our simple model, this peak represents the ‘‘multiplet structure’’ associated with the TM element. It will evolve into a genuine multiplet upon inclusion in the model of more orbitals at the TM site.

Correlations at the O site have similar effects, as shown in Fig. 3(b). Since the cost of removing an electron from the O ion is now lowered by  $U_O$ , the central band shifts by an additional  $-U_O$ , while the upper band shifts by an additional  $-2U_O$ . On the other hand, the lowest band with the two holes in the TM-like band is essentially unchanged, while the multiplet peak is shifted to slightly lower energies due to level repulsion with the central continuum. Correlations at O sites also produce an (anti)bound discrete state with both holes at the same O site which is pushed above the upper continuum. However, it has very little weight and can only be seen on a greatly expanded

scale, as shown in the inset, as a small peak located just above the highest-energy band edge.

To summarize, the location of the continua in the momentum-resolved AES spectrum must agree with the self-convolution of the one-hole spectrum, which can be obtained from angle-resolved photoemission spectroscopy (ARPES). Additional discrete peaks (or strong sharp resonances, if these happen to fall inside another continuum) indicate the presence of on-site correlations, and allow one to find various on-site parameters from the corresponding multiplet structure.<sup>28</sup> Of course, because the projection is on the  $|k, 0, dd\rangle$  state, the spectral weight is large for states which predominantly have both holes at the same TM site. As discussed in the previous section, it is trivial with our method to project on other states, for example, with both holes at the same O site. While the spectrum is unchanged, this will shift the spectral weight between the different features.

### B. Variational approximation

In Figs. 4 and 5, we present data obtained with our variational approximation for the same sets of parameters. As before, the vertical markers show the expected location of the band edges, based on the convolution of the one-hole spectra.

Starting with the uncorrelated case in Fig. 4, we see that this variational approximation is very poor when  $\Delta = 0$ , in Fig. 4(a). While the overall spectral range is in fair agreement with that predicted by the two-hole convolutions, inside this interval there is significant disagreement. In particular, the variational calculation predicts spectral weight at energies that should be gapped. This disagreement is not surprising, since in this case we are projecting out states that have energies very similar to the states we keep, and this is not a sensible strategy.

As shown in Figs. 4(b) and 4(c), the situation improves when  $\Delta$  is large enough to separate a TM-like band from the O-like band. In this case, the agreement for the two less visible bands is reasonable, even though the projection may slightly over/underestimate the location of the band edges and it produces additional structure within the bands, especially the central one. This is not surprising since one expects a fair amount of hybridization between states in the central continuum, which have one hole in the TM-like band and one in the O-like band, with the states with the two holes at different TM sites that are projected out.

Finally, the continuum with the two holes in the TM-like bands is replaced by discrete peaks located at roughly the correct energy. The disappearance of this continuum is expected, since we projected out precisely the states responsible for generating it, i.e., with holes at different TM sites. In the absence of correlations, the state with both holes at the same TM site has a similar energy, hence the peak. Similar conclusions hold for  $\Delta = -5$ .

If we turn on the correlations, this multiplet-structure peak moves away from the continuum. Indeed, as shown in both panels of Fig. 5, now the low-energy continuum with the two holes in the TM-like band is completely absent from the variational results, but the important feature, i.e., the high-weight multiplet-structure peak, is essentially indistinguishable from that predicted by the full solution. The higher-energy continua show some additional structure within

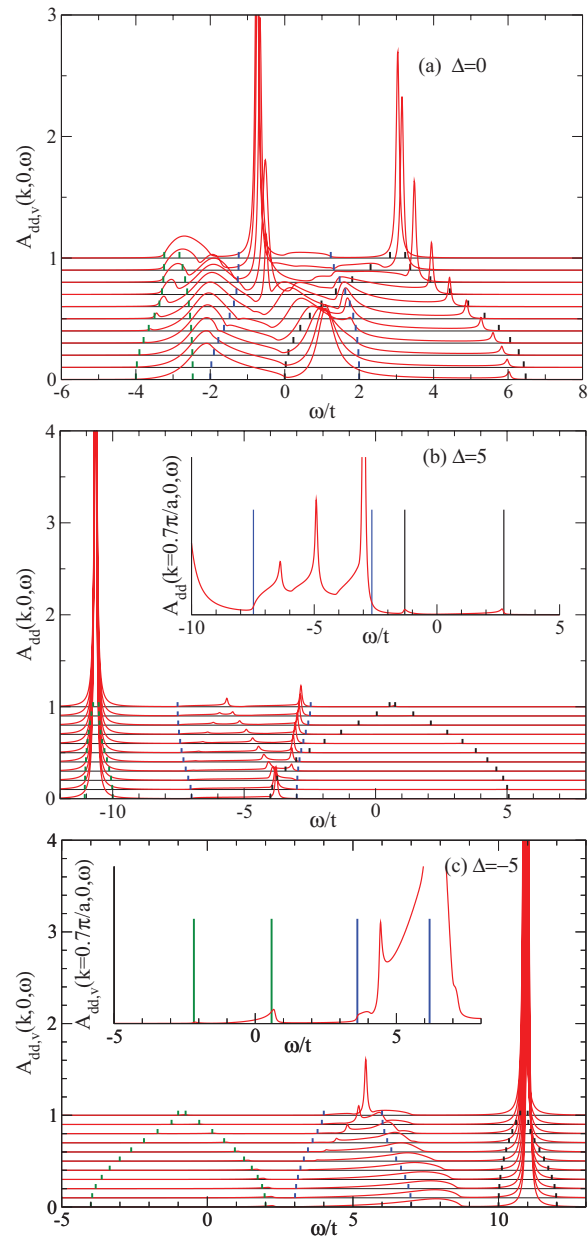


FIG. 4. (Color online) Same as in Fig. 2, but the AES spectral weight is obtained with the variational approximation.

this variational calculation, but since this structure also appears in the absence of correlations, there is little danger of confusing it with real features induced by the correlations.

To summarize, for parameters likely relevant for the real materials, i.e., when the TM-like and O-like bands are sufficiently well separated, the variational approximation does a very good job of capturing the multiplet structure due to TM on-site correlations. One of the continua is projected out, but it has little weight and its location is *a priori* known from the one-hole spectrum. The higher-energy continua are reproduced at roughly the correct locations, but with some additional features, which, however, also appear in the absence of correlations. With some care, one can use this more efficient calculation to understand most, if not all, of the important physics contained within these spectra.

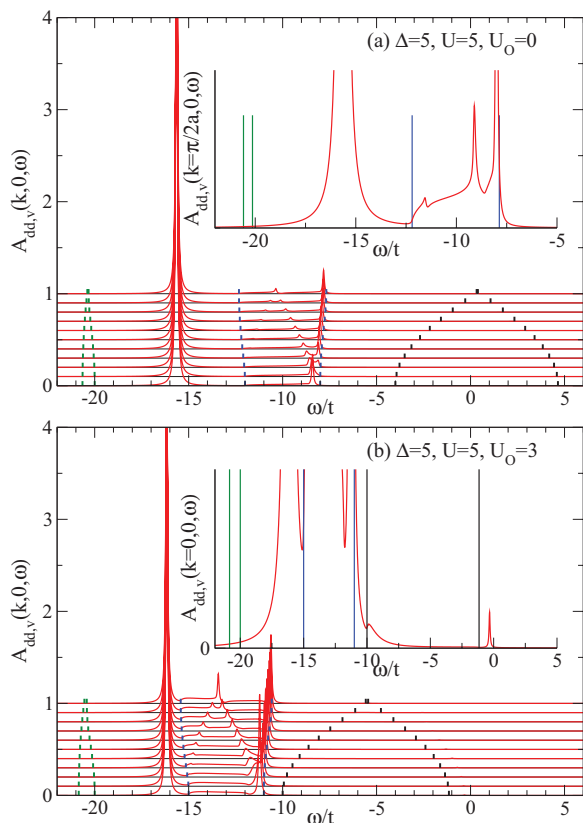


FIG. 5. (Color online) Same as in Fig. 3, but the AES spectral weight is obtained with the variational approximation.

### C. Impurity approximation

For comparison, we also present AES spectra obtained with the impurity approximation. Since here the translational invariance is lost, we can only show one  $A_{dd}(\omega)$  curve for each set of parameters. This can be roughly thought of as a momentum-integrated spectral weight.

(1) Trivial topology: We begin with the simpler impurity model sketched in Fig. 6(a), where the TM impurity is connected to two independent semi-infinite half chains.

If  $\Delta$  is sufficiently large, the single-hole spectrum consists of a discrete peak (hole localized at TM site) and a continuum (hole in the O-band). As a result, the two-hole convolution consists of three features: (i) a discrete state with both holes at

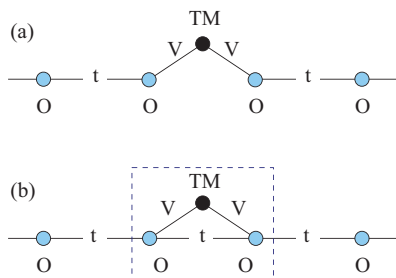


FIG. 6. (Color online) Two ways to connect the impurity to the O bath: (a) trivial and (b) nontrivial topology. The latter can be reduced to the former if one considers the three central ions enclosed by the box to form an effective “impurity.”

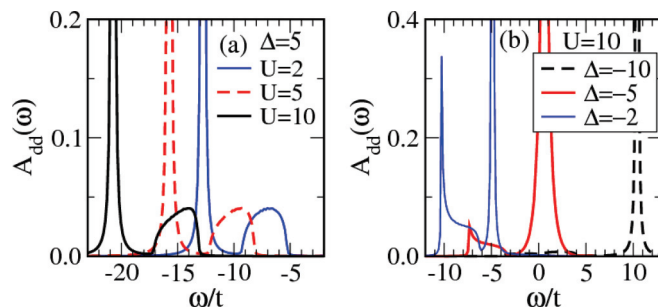


FIG. 7. (Color online) Impurity spectral function  $A_{dd}(\omega)$  vs  $\omega$  for the trivial topology of Fig. 6(a) with  $t = V = 1$  and (a)  $\Delta = 5$ ,  $U = 2, 5, 10$ ,  $U_O = 0$ , and (b)  $\Delta = -10, -5, 2$ ,  $U = 5$ ,  $U_O = 0$ .

the TM site (the multiplet), (ii) a continuum of states with one hole occupying the TM impurity state and the other moving freely in the O bath, and (iii) the two-hole continuum with both holes in the O bath, which here spans the interval  $[-2U_O - 4t, -2U_O + 4t]$ , irrespective of the value of  $V$ .

Results shown in Fig. 7 for several sets of parameters indeed show these features, although the two-hole continuum can only be observed on a magnified scale.

(2) Nontrivial topology: Results for similar parameters, but for the nontrivial topology of Fig. 6(b), are shown in Fig. 8. Here the impurity forms a ring with its two neighbor O sites. This nontrivial topology can support more impurity states localized on the ring than the trivial topology discussed above, so one may expect a more complex two-hole spectrum.

In Fig. 8(a), we plot  $A_{dd}(\omega)$  for  $t = V = 1$ ,  $U = U_O = 0$ , and  $\Delta = 0, 5$ . The  $\Delta = 0$  spectrum shows two broad resonances in the two-hole continuum plus a discrete peak above it. These are understood in terms of the ring multiplet. For these parameters, the isolated ring has three two-hole eigenstates at  $-2t, t, 4t$ . The two broad resonances are associated with the former two, while the latter falls at the upper edge of the continuum and is pushed above it by level repulsion. States with one hole on the ring and the other in the bath overlap with the two-hole continuum. For  $\Delta = 5$  (thick black line), there are two one-hole ring eigenstates at  $-5.32t, 1.32t$ , resulting in three two-hole ring eigenstates at  $-10.63t, -4t, 2.63t$ . The latter two fall inside the two-hole continuum, so only the former is visible as a discrete peak. The continua with one hole on the ring and one in the bath span  $[-7.32t, -3.32t]$  and  $[-0.68t, 3.32t]$ , respectively. Only the former is (partially)

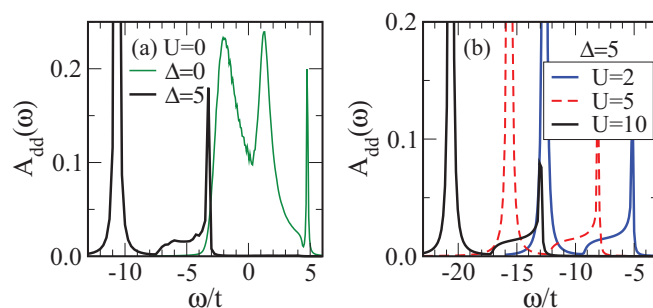


FIG. 8. (Color online) Impurity spectral function  $A_{dd}(\omega)$  vs  $\omega$  for the nontrivial topology of Fig. 6(b) with  $t = V = 1$  and (a)  $\Delta = 0, 5$  and  $U = U_O = 0$ , (b)  $\Delta = 5$ ,  $U = 2, 5, 10$ ,  $U_O = 0$ .

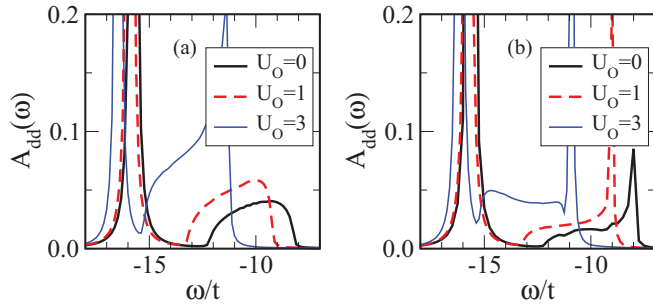


FIG. 9. (Color online) Impurity spectral function  $A_{d\uparrow,d\downarrow}(\omega)$  vs  $\omega$  for (a) the trivial topology and (b) the ring topology, with  $t = V = 1$ ,  $\Delta = U = 5$ , and  $U_O = 0, 1, 3$ .

distinct from the two-hole continuum, and is visible in the spectrum. Very little weight is left in the two-hole continuum, which is not visible on this scale. The effect of correlations, shown in Fig. 8(b), can be explained with similar arguments.

Interestingly, these results are qualitatively like those of Fig. 7(a) for the trivial topology because the additional states in the ring multiplet fall inside the two-hole continuum and are washed out into broad, low-weight resonances. This is certainly true for  $U \gg t, |\Delta| \gg t$ , when the TM states become (to zero order in perturbation theory) eigenstates of the ring, with the remaining ring eigenstates involving only O sites and therefore being located inside the two-hole continuum.

(3) Bath correlation effects: In Fig. 9, we briefly show the effect of adding on-site repulsion at the O sites in the impurity approximation. Figure 9(a) is for the trivial topology while Fig. 9(b) is for the ring topology. The main effect of  $U_O$  is to shift the continuum with one hole in the bath to lower energies by  $U_O$ , as expected. This leads to a stronger hybridization with the discrete peak, which is consequently pushed to lower energies as well. The weights in these features also vary, but the two-hole continuum remains invisible on this scale.

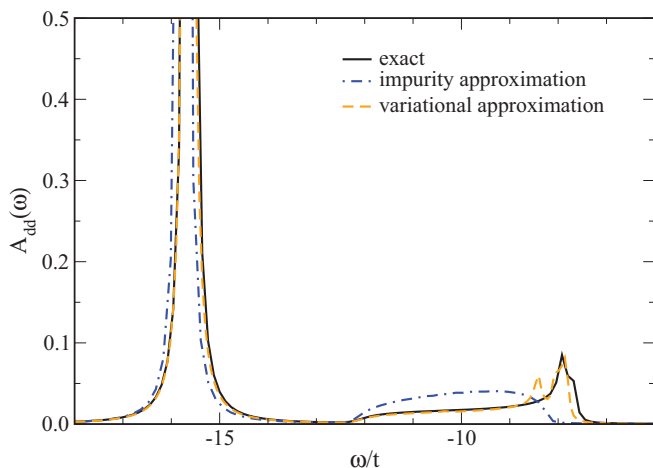


FIG. 10. (Color online) Momentum-integrated AES spectral weight  $\frac{1}{N} \sum_k A_{dd}(k, \omega)$  for the exact solution (full line) and our variational approximation (dashed line) compared to the prediction of the impurity approximation with trivial topology (dot-dashed line), for  $t = V = 1$ ,  $U = \Delta = 5$ ,  $U_O = 0$ .

To summarize, we find that the results for the two topologies are rather similar if  $|\Delta|$  and/or  $U$  are large compared to  $t, V$  (if this is not the case, the impurity approximation is not valid). In this limit, the impurity approximation is quite successful in reproducing the location of the multiplet peak, as shown in Fig. 10 where we compare  $A_{dd}(\omega)$  for the trivial topology (dot-dashed line) against  $\frac{1}{N} \sum_k A_{dd}(k, \omega)$  for the exact solution (full line) and our variational approximation (dashed line) for  $\Delta = U = 5, U_O = 0$ . The multiplet peak disperses very weakly for these parameters so all three curves show what looks like a discrete peak at low energies. As expected, the variational approximation provides a more accurate estimate of the peak position. The impurity approximation is also less successful in predicting the correct bandwidth for the continuum visible at higher energies; when analyzing experimental data, this may result in wrong values assigned to the hopping parameters. Figure 10 confirms that our variational approximation is more accurate than the impurity approximation.

## V. DISCUSSION AND CONCLUSIONS

In this work, we introduced a variational approach to calculate two-hole Green's functions needed for AES spectroscopy and applied it to a simple 1D model with otherwise full bands, so that we can compare its predictions against the exact solution available for this case. We also calculated the results in the impurity approximation for two different ways of connecting the impurity to the O bath.

Both approximations are reasonable to use only if the single-electron parameters are such that one-hole eigenstates with the hole primarily at the TM site (i.e., of TM character) are energetically well separated from those with the hole primarily in the O band. If this is not true, then the basis states projected out in these approximations are energetically close to those kept within the calculation, and the results are not sensible.

If the above-mentioned condition is satisfied, our variational approximation is superior to the impurity approximation. Not only does it produce momentum-resolved results, but the location of the continua that appear in the AES spectrum is in fair agreement with that expected from the convolution of the one-hole spectra, unlike for the impurity approximation. The superiority of our method can also be justified as follows: both methods are variational, since both limit the basis of allowed two-hole states. Our method has a much bigger variational space, therefore it has to be more accurate. The results presented here confirm it.

Since the one-hole spectrum can be obtained from ARPES measurements (and, from a theoretical perspective, can be calculated with methods analogous to those we use here to find the two-hole propagator), a combination of the two spectroscopies can be used to determine which features in the two-hole spectrum come from this convolution. Any other features must be due to on-site correlations, and can therefore help pinpoint the values of various on-site interaction energies.

The method of Ref. 25 can be extended straightforwardly to compute Green's functions for problems with three or more holes. As a result, it can certainly be used to solve impurity-type problems where the TM has a partially filled  $d$  shell while



the O band is completely full prior to the Auger process. If the TM has a  $3d^n, n < 10$ , configuration, then after the Auger process there are  $12 - n$  holes in the impurity problem. While computational times depend on  $n$  and on how complicated the O bath is (how many  $2p$  orbitals per O, and in what dimension), at least some of the higher- $n$  cases should be solvable exactly. One can make further progress using the fact that processes where very many more than two holes hop into the O bath should be energetically very costly (otherwise, the ground state would have partially filled O bands to begin with). As a result, one could systematically increase the number of holes allowed to hop into the bath starting from two, until convergence is reached. This may allow one to investigate all possible  $n$  values within the impurity approximation, if convergence is reached fast enough.

Similar considerations apply to our variational method, because the total number of basis states it includes (for each fixed value of  $k$ ) is smaller but comparable to that for the impurity approximation. As a result, one should get more accurate and momentum-resolved results at comparable computational costs.

Of course, not all oxides have full O  $2p$  bands, although many do for at least some particular doping (e.g., an insulating parent compound). We envision using this method to extract information about crystal-field splitting and on-site and nearest-neighbor interactions from Auger spectroscopy on this compound. If further doping that results in partially filled O  $2p$  bands does not result in significant additional screening of these short-range interactions, then these values would be relevant over the entire doping range.

In conclusion, we believe that this method proposes an efficient way to make progress on understanding AES spectra for systems where the  $d$  orbitals of the TM are only partially filled, so long as the states of TM character are not too close to the filled O states. Such work is now in progress.

## ACKNOWLEDGMENTS

This work was supported by NSERC, CIFAR, and QMI.

## APPENDIX A: CONTINUED-FRACTION SOLUTION FOR THE IMPURITY APPROXIMATION

For technical reasons which will become apparent soon, it is more convenient to group the TM and the two O sites it directly hybridizes with together into “site” 0, and to index the O atoms to its right/left as  $\pm 1, \pm 2$ , etc. The two O inside site 0 will be called “a” and “b,” respectively. This indexing is shown in Fig. 11. Amongst other things, this indexing makes it easy to study the two situations depicted in Figs. 11(a) and 11(b), where the hopping between the two central O is turned off/on.

We use the operator identity  $(\omega + E_\Omega^I + i\eta - \mathcal{H}_I)\hat{G}_I(\omega) = \hat{I}$  to generate EOMs for the Green’s functions. For example, for any  $|i| > 1, |j| > 1$ , this results in  $[\omega + E_\Omega^I + U_O(2 - \delta_{i,j}) + i\eta]G_{i\uparrow,j\downarrow}(\omega) = tG_{i\uparrow,j+1\downarrow}(\omega) + tG_{i-1\uparrow,j\downarrow}(\omega) + tG_{i\uparrow,j-1\downarrow}(\omega) + tG_{i+1\uparrow,j\downarrow}(\omega)$ , where  $G_{i\sigma,j\sigma'}(\omega) = \langle dd|\hat{G}_I(\omega)|i\sigma,j\sigma'\rangle$ . In other words, it links together propagators where the holes are at a distance  $|i - j| = n$

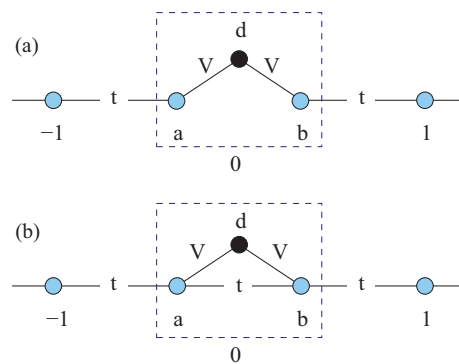


FIG. 11. (Color online) Actual indexing of the O sites used in this work. The three central atoms comprise “site” 0.

apart to propagators where the holes are  $n \pm 1$  sites apart. This allows us to rewrite these equations of motion as simple recurrence relations by grouping together in a vector  $V_n$  all the propagators where the holes are  $n$  sites apart. Note that this is true for states with a hole at site 0 and one at any site  $|n| \geq 1$ , which also enter into  $V_n$  and only link to propagators in  $V_{n\pm 1}$ .

To be more precise, let

$$V_n^{\sigma,\sigma'} = \begin{pmatrix} \cdot \\ \cdot \\ \cdot \\ G_{i\sigma;i+n,\sigma'}(\omega) \\ G_{i-1,\sigma;i+n-1,\sigma'}(\omega) \\ G_{i-2,\sigma;i+n-2,\sigma'}(\omega) \\ \cdot \\ \cdot \\ \cdot \end{pmatrix}$$

be a vector of infinite length which contains all the propagators with the holes  $n$  sites apart. Of course, there are three entries replacing the  $(0,n)$  entry, corresponding to sites  $a,b,d$ , and similarly for  $(-n,0)$ . Further, we note that for  $n \geq 1$ , the ordering of the spins is preserved under hopping, since the leftmost hole cannot pass by the rightmost hole with one hop. Thus, we can write a recurrence relation for these vectors, for any  $n \geq 1$ , as

$$\begin{pmatrix} \gamma_n & 0 \\ 0 & \gamma_n \end{pmatrix} \begin{pmatrix} V_n^{\uparrow\downarrow} \\ V_n^{\downarrow\uparrow} \end{pmatrix} = \begin{pmatrix} \alpha_n & 0 \\ 0 & \alpha_n \end{pmatrix} \begin{pmatrix} V_{n-1}^{\uparrow\downarrow} \\ V_{n-1}^{\downarrow\uparrow} \end{pmatrix} + \begin{pmatrix} \beta_n & 0 \\ 0 & \beta_n \end{pmatrix} \begin{pmatrix} V_{n+1}^{\uparrow\downarrow} \\ V_{n+1}^{\downarrow\uparrow} \end{pmatrix}, \quad (\text{A1})$$

where  $\gamma_n, \alpha_n$ , and  $\beta_n$  are very sparse matrices, whose elements can be read off from the equations of motion as in the periodic case. Further, as before, the tridiagonal form of the recurrence relation admits a continued fraction solution for these vectors. The rest of the procedure is the same as for the periodic case.

### 1. Truncation schemes of continued fractions

(i) For this method to work, we need to truncate the continued fraction at a large interhole separation  $M$ , both for

the periodic and impurity cases. In the periodic system, we start out by creating two holes on a TM site. The two holes can now delocalize in the system. However, the broadening  $\eta$  introduces a finite lifetime ( $\sim 1/\eta$ ) so that  $\langle k, 0, dd | G_P(\omega) | k, n, \alpha\beta \rangle \rightarrow 0$  as  $n \rightarrow \infty$ . Thus, for a large enough  $n = M$ , we can truncate the continued fraction for the  $V$  vectors by setting  $V_{M_c+1}$  to zero.

For the impurity problem, this is justified because  $G_{i\sigma;i+n,\sigma'}(\omega)$  is the Fourier transform of the amplitude of probability that the two holes move from the impurity (TM) site to the sites  $i, i+n$  within a time  $\tau$ . The larger  $n$  is, the less likely this process becomes, hence the smaller these propagators must be. This is certainly true for the energy ranges spanned by eigenstates that favor having the holes on the impurity (TM) site, since then they are unlikely to wander very far away from it. However, this is also true even if the holes preferred the O bath. This is because the broadening  $\eta$  is equivalent to introducing a finite lifetime  $\sim 1/\eta$  for the holes, so they cannot move arbitrarily far in a finite time  $\tau$ . Of course, in this latter case, the appropriate cutoff  $M$  increases as  $\eta$  decreases. In practice, for both cases, we increase  $M$  until the results become insensitive to further changes.

(ii) A further truncation is necessary for the impurity problem. This is because, with the ordering of the propagators used for the  $V_n$  vectors, we have the additional complication that all of these vectors, and therefore all of the sparse matrices  $\alpha_n, \beta_n, \gamma_n$ , are infinitely dimensional. In order to calculate the continued fractions, we need to truncate the size of these vectors, as well. The reasons discussed above justify doing this if  $|i| \gg 1$  and/or  $|i+n| \gg 1$ . We use the following truncation procedure: for a fixed separation  $n$  between the holes, the maximum distance that either of the two holes is allowed to travel away from the TM is  $R_c + n$ , i.e., we truncate  $V_n^{\sigma,\sigma'}$  at  $G_{R_c,\sigma;R_c+n,\sigma'}(\omega)$  at the top and  $G_{-R_c-n+1,\sigma;-R_c+1,\sigma'}(\omega)$  at the bottom. Again,  $R_c$  is increased until results become independent of its value. As a final comment, we note that there are other ways of grouping the propagators into vectors so that the equations of motion still lead to a simple recursive relation. Different schemes have various computational advantages and disadvantages, but they all converge to the correct answer if the cutoffs are sufficiently large. This converged result is equivalent to the exact solution computed

by the Cini-Sawatzky theory for the Anderson impurity problem.

## APPENDIX B: CHOICE OF PARAMETERS

For simplicity, we discuss the impurity approximation first and the full periodic system second.

For the impurity approximation, if we ignore the TM-bath hybridization,  $V \rightarrow 0$ , then if both holes are at the TM site, the energy of the state is  $E_\Omega^I - 2\Delta - U$ ; if one hole is at the TM site and one is in the O bath, the minimum energy of such states is  $E_\Omega^I - \Delta - U - 2t - U_O$ . Finally, if both holes are in the O bath, the minimum energy of such states is  $E_\Omega^I - 4t - 2U_O$ . As a result, the state with both holes at the TM atom is favorable energetically if  $\Delta > 2t + U_O$  and  $2\Delta + U > 4t + 2U_O$ . The second condition is automatically satisfied if the first one holds, since the TM on-site interaction is repulsive,  $U > 0$ .

The condition  $\Delta > 2t + U_O$  implies that AES should be more useful for Mott insulators than for charge-transfer materials.<sup>29</sup> To see this, consider one-electron removal states from the ground state (GS). If the hole is removed from the TM site, the energy of the state is  $E_\Omega^I - \Delta - U$ , while if it is removed from an O site, the minimum energy is  $E_\Omega^I - 2t - U_O$ . The latter is energetically more expensive than the former if  $\Delta > 2t + U_O$ . This makes sense because if the material was a charge-transfer insulator, the additional holes would prefer to stay in the O bath and AES would be less sensitive to the TM-atom-specific properties.

The analysis for the periodic system is very similar for  $V \rightarrow 0$  because the energy differences between states having (i) both holes at the same TM site, (ii) one hole at a TM site and one in the O bath, and (iii) both holes in the O bath are precisely the same as for the impurity case. Because of this and also in order to be able to meaningfully compare with impurity approximation results, we use the same parameters in both cases.

Note that in the periodic system, we can also have (iv) the two holes at different TM sites. For  $V = 0$ , these states have energy  $E_\Omega^P - 2\Delta - 2U$  and are always energetically favored compared to having both holes at the same TM site. Of course, these are the states projected out in our variational calculation.

<sup>1</sup>B. Feuerbacher, B. Fitton, and R. Willis, *Photoemission and the Electronic Properties of Surfaces* (Wiley, New York, 1978).

<sup>2</sup>D. Chattarji, *The Theory of Auger Transitions* (Academic, New York, 1976).

<sup>3</sup>E. Antonides, E. C. Janse, and G. A. Sawatzky, *Phys. Rev. B* **15**, 1669 (1977).

<sup>4</sup>D. E. Ramaker, *Crit. Rev. Solid State Mater. Sci.* **17**, 211 (1991).

<sup>5</sup>L. C. Davis, *J. Appl. Phys.* **59**, R25 (1986).

<sup>6</sup>J. Ghijsen, L. H. Tjeng, J. van Elp, H. Eskes, J. Westerink, G. A. Sawatzky, and M. T. Czyzyk, *Phys. Rev. B* **38**, 11322 (1988).

<sup>7</sup>M. Cini, *Solid State Commun.* **24**, 681 (1977).

<sup>8</sup>M. Cini, *Solid State Commun.* **20**, 605 (1976).

<sup>9</sup>G. A. Sawatzky, *Phys. Rev. Lett.* **39**, 504 (1977).

<sup>10</sup>M. Potthoff, in *Band-Ferromagnetism*, Lecture Notes in Physics, Vol. 580 (Springer, Berlin-Heidelberg, 2001), pp. 356–370.

<sup>11</sup>M. Cini, *Phys. Rev. B* **17**, 2486 (1978).

<sup>12</sup>M. Cini and A. D'Andrea, *Phys. Rev. B* **29**, 6540 (1984).

<sup>13</sup>M. Cini, *Phys. Rev. B* **32**, 1945 (1985).

<sup>14</sup>C. Verdozzi and M. Cini, *Phys. Rev. B* **51**, 7412 (1995).

<sup>15</sup>M. Cini, A. Parnascelci, and E. Paparazzo, *J. Electron Spectrosc. Relat. Phenom.* **72**, 77 (1995).

<sup>16</sup>A. Parnascelci and M. Cini, *J. Electron Spectrosc. Relat. Phenom.* **82**, 79 (1996).

<sup>17</sup>P.-O. Löwdin, *J. Chem. Phys.* **18**, 365 (1950).

<sup>18</sup>O. Gunnarsson, K. Schönhammer, J. C. Fuggle, and R. Lässer, *Phys. Rev. B* **23**, 4350 (1981).

- <sup>19</sup>C. Verdozzi, M. Cini, and A. Marini, *J. Electron Spectrosc. Relat. Phenom.* **41**, 117 (2001).
- <sup>20</sup>A. Marini and M. Cini, *Phys. Rev. B* **60**, 11391 (1999).
- <sup>21</sup>P. W. Anderson, *Phys. Rev.* **124**, 41 (1961).
- <sup>22</sup>O. Gunnarsson and K. Schönhammer, *Phys. Rev. B* **28**, 4315 (1983).
- <sup>23</sup>J. Zaanen, C. Westra, and G. A. Sawatzky, *Phys. Rev. B* **33**, 8060 (1986).
- <sup>24</sup>H. Eskes and G. A. Sawatzky, *Phys. Rev. B* **44**, 9656 (1991).
- <sup>25</sup>M. Berciu, *Phys. Rev. Lett.* **107**, 246403 (2011).
- <sup>26</sup>M. Möller, A. Mukherjee, C. P. J. Adolphs, D. J. J. Marchand, and M. Berciu, *J. Phys. A: Math. Theor.* **45**, 115206 (2012).
- <sup>27</sup>M. Berciu and A. M. Cook, *Europhys. Lett.* **92**, 40003 (2010).
- <sup>28</sup>E. Antonides, E. C. Janse, and G. A. Sawatzky, *Phys. Rev. B* **15**, 4596 (1977).
- <sup>29</sup>J. Zaanen, G. A. Sawatzky, and J. W. Allen, *Phys. Rev. Lett.* **55**, 418 (1985).